Optical absorption in asymmetrical Gaussian potential quantum dot under the application of an electric field*

Xue-Chao Li(李学超), Chun-Bao Ye(叶纯宝)†, Juan Gao(高娟), and Bing Wang(王兵)

Optoelectronics Physics, Anhui University of Science and Technology, Huainan 232001, *China*

(Received 23 February 2020; revised manuscript received 13 April 2020; accepted manuscript online 13 May 2020)

We theoretically investigate the optical absorption coefficient (OAC) in asymmetrical Gaussian potential quantum dots subject to an applied electric field. Confined wave functions together with energies of electron energies in an effective mass approximation framework are obtained. The OAC is expressed according to the iterative method and the compact-density-matrix approach. Based on our results, OAC is sensitively dependent on external electric field together with the incident optical intensity. Additionally, peak shifts into greater energy as the quantum dot radius decrease. Moreover, the parameters of Gaussian potential have a significant influence on the OAC.

Keywords: electric field, optical absorption, quantum dot

PACS: 73.21.La, 94.20.Ss, 33.80.–b **DOI:** 10.1088/1674-1056/ab9284

1. Introduction

Recently, many low-dimensional semiconductor systems including quantum dots (QDs) and other confined nanostructures have been studied. Due to the discrete energy levels and unique optical characters, much attention has been focused on both colloid QDs[1–4] and self-assembly QDs.[5,6] Compared with bulk materials, confined nanostructures have significantly different nonlinear optical properties.[7–10] Particularly, electric field application has been extensively studied for the semiconductor nanostructures.[11–13] In recent years, tremendous efforts are made to examine those optical as well as electronic characteristics for QDs, where carrier motion is restricted at each spatial direction. External static electric field can modify electron optical properties and transport within QDs. The electric field applied can result in carrier distribution polarization, along with quantum state energy shift, where the intensity of optoelectronic devices can be controlled and modulated effectively. Therefore, the electric field effect on the carrier within QDs deserves investigation.

The optical absorption coefficient (OAC) with semiconductor nanostructures has aroused wide attention over the last few years.[14–16] Many researchers considered the electric field effect when investigating the OAC. For instance, Mandal *et al.*[17] have studied the OAC of QDs under noise, electric and magnetic fields, confinement potential. Zhang *et al.*[18] have investigated the OAC and the refractive index changes within the asymmetrical Gaussian potential quantum well in the presence of an applied external electric field. Çakır *et al.*[19] reported the magnetic field impacts on linear and nonlinear OACs in spherical QDs. Ghajarpour *et al.*[20] examined hydrogenic impurity, magnetic and electric fields on the OAC within QDs. Al *et al.*[21] have analyzed the electric field impacts on the binding energy and the OAC within the Tietz-Hua quantum well. In all the above-mentioned articles, authors proposed electric and magnetic fields, the external perturbation on the OAC. In this paper, we mainly investigate the OAC within an asymmetrical Gaussian potential QD when an external electric field is applied, although extreme nonlinear optics is another important research hotspot of nonlinear optics and a lot of important research results have been obtained.[22–25]

The numerical research on the OAC within the asymmetrical Gaussian potential QD when an external electric field is applied is presented in this study. To be specific, a theoretical framework is presented in Section 2. Section 3 presents the numerical discussion of findings, and Section 4 presents the conclusions.

2. Model and analysis

In the effective mass approximation framework, the Schrödinger equation of the system is given by[26,27]

$$\hat{H}\Psi = \left[\frac{\boldsymbol{P}^2}{2m^*} + \frac{1}{2}m^*\omega_0^2\rho^2 + V(z) + eFz\right]\Psi, \tag{1}$$

where m^* stands for effective mass of the electron in the conduction band, and $\omega_0 = \hbar/m^*R^2$ represents electron frequency, R indicates QD radius, F is electric field magnitude. The asymmetrical Gaussian potential $V(z)$ is

$$V(z) = \begin{cases} -V_0 \exp\left(-\dfrac{z^2}{2L^2}\right), & z \geq 0, \\ \infty, & z < 0, \end{cases} \tag{2}$$

*Project supported by the National Natural Science Foundation of China (Grant Nos. 51702003, 61775087, and 11674312), the Provincial Foundation for Excellent Top Talents of Colleges and Universities of Anhui Province of China (Grant No. gxgwfx2019016), the Anhui Provincial Natural Science Foundation, China (Grant Nos. 1808085ME130 and 1508085QF140), University Outstanding Young Talents Support Program Fund (Grant No. gxyqZD2018039).

†Corresponding author. E-mail: cbyeaust@163.com

where V_0 stands for the Gaussian potential barrier height, and L indicates the confinement potential range. First of all, the related system eigenfunctions are shown as follows:

$$\Psi = f(\rho,\varphi)\chi(z), \tag{3}$$

$$f(\rho,\varphi) = \frac{1}{a^{1+|m|}}\sqrt{\frac{(n+|m|)!}{2\pi 2^{|m|}n!}}\frac{1}{m!}\exp(\mathrm{i}m\varphi)\rho^{|m|} \times \exp\left(-\frac{\rho^2}{4a^2}\right)F\left(-n,1+|m|,\frac{\rho^2}{2a^2}\right), \tag{4}$$

$$\chi_{n_z}(z) = \sqrt{\frac{\alpha}{2^{n_z}n_z!\sqrt{\pi}}}\exp\left(-\frac{\alpha^2 z^2}{2}\right) \times H_{n_z}\left[\alpha\left(z-\frac{eFL^2}{V_0}\right)\right], \tag{5}$$

where $\alpha = \frac{(m^*V_0)^{1/4}}{(\hbar L)^{1/2}}$, $a = \sqrt{\frac{\hbar}{2m^*\omega_0}}$ stands for scale of effective length, $F(a,b,x)$ represents the confluent hypergeometric function, n_z is the number of quantum, n represents the number of radial quantum, whereas $H_{n_z}(z)$ stands for Hermite polynomials.

In addition, electron eigenenergies E is determined according to the equation

$$E = 2\hbar\omega_0\left(n+\frac{1}{2}\right)+\left(2n_z+\frac{3}{2}\right)\frac{\hbar}{L}\sqrt{\frac{V_0}{m^*}} - V_0 - \frac{e^2F^2L^2}{2V_0}. \tag{6}$$

By adopting the iterative method and the compact-density-matrix approach, the OAC formula within the QD is calculated. Assume that our system can be triggered via an applied electromagnetic field, whose electric field vector can be expressed as

$$E(t) = \widetilde{E}\,\mathrm{e}^{-\mathrm{i}\omega t}+\widetilde{E}^*\,\mathrm{e}^{\mathrm{i}\omega t}, \tag{7}$$

where ω stands for external incident field frequency. Thereafter, the density matrix operator ρ evolution is determined by the Schrödinger equation dependent on time

$$\frac{\partial\rho_{ij}}{\partial t} = \frac{1}{\mathrm{i}\hbar}[H_0 - qzE(t),\rho]_{ij} - \Gamma_{ij}\left(\rho-\rho^{(0)}\right)_{ij}, \tag{8}$$

where H_0 indicates the system Hamiltonian in the absence of light field $E(t)$, Γ_{ij} represents relaxation time, and $\rho^{(0)}$ stands for the unperturbed density matrix. Eqation (8) can be determined based on the iterative approach as follows:

$$\rho(t) = \sum_n \rho^n(t) \tag{9}$$

with

$$\frac{\partial\rho_{ij}^{(n+1)}}{\partial t} = \frac{1}{\mathrm{i}\hbar}\left\{\left[H_0,\,\rho^{(n+1)}\right]_{ij} - \mathrm{i}\hbar\Gamma_{ij}\rho_{ij}^{(n+1)}\right\} - \frac{1}{\mathrm{i}\hbar}\left[qz,\,\rho^{(n)}\right]_{ij}E(t). \tag{10}$$

The QD electric polarization is expanded as follows:

$$P(t) = \varepsilon_0\chi^{(1)}\widetilde{E}\,\mathrm{e}^{-\mathrm{i}\omega t}+\varepsilon_0\chi_0^{(2)}|\widetilde{E}|^2+\varepsilon_0\chi_{2\omega}^{(2)}\widetilde{E}^2\,\mathrm{e}^{-\mathrm{i}2\omega t} +\varepsilon_0\chi_{3\omega}^{(3)}\widetilde{E}^3\,\mathrm{e}^{-\mathrm{i}3\omega t}+\mathrm{c.c.}, \tag{11}$$

where $\chi^{(1)}$, $\chi_0^{(2)}$, $\chi_{2\omega}^{(2)}$, and $\chi_{3\omega}^{(3)}$ represent the linear susceptibility, optical rectification, coefficient of second-harmonic generation, as well as susceptibility of third-harmonic generation, respectively. In addition, ε_0 indicates vacuum dielectric constant. Moreover, the n-th order electronic polarization can be calculated by

$$P^{(n)}(t) = \frac{1}{V}\mathrm{Tr}\left(\rho^{(n)}ez\right), \tag{12}$$

where V stands for interaction volume, whereas Tr is summation or trace over matrix diagonal elements $\rho^{(n)}ez$.

Within the iterative and compact-density matrix approaches, the analytical expressions for the linear and third-order nonlinear susceptibilities are calculated by[28,29]

$$\alpha^{(1)}(\omega) = \omega\sqrt{\frac{\mu}{\varepsilon_\mathrm{R}}}\frac{|M_{21}|^2\sigma_v\hbar\Gamma_{12}}{(E_{21}-\hbar\omega)^2+(\hbar\Gamma_{12})^2}, \tag{13}$$

$$\alpha^{(3)}(\omega,I) = -\omega\sqrt{\frac{\mu}{\varepsilon_\mathrm{R}}}\left(\frac{I}{2\varepsilon_\mathrm{R}n_\mathrm{r}c}\right)\times\frac{|M_{21}|^2\sigma_v\hbar\Gamma_{12}}{[(E_{21}-\hbar\omega)^2+(\hbar\Gamma_{12})^2]^2}\left[4|M_{21}|^2-\frac{|M_{22}-M_{11}|^2[3E_{21}^2-4E_{21}\hbar\omega+\hbar^2(\omega^2-\Gamma_{12}^2)]}{E_{21}^2+(\hbar\Gamma_{12})^2}\right]. \tag{14}$$

For the above-mentioned equations, μ stands for the system permeability, ε_R represents the actual permittivity, ε_0 suggests the free space permittivity, I indicates incident optical intensify, c indicates light speed, n_r represents refractive index, $M_{ij} = |\langle\Psi_i|ez|\Psi_j\rangle|(i,j=1,2)$, $E_{ij} = E_i - E_j$ suggests an energy interval between two distinct electronic states. Moreover, the overall coefficients of optical absorption are expressed as

$$\alpha(\omega,I) = \alpha^{(1)}(\omega)+\alpha^{(3)}(\omega,I). \tag{15}$$

3. Results and discussion

This section introduces the third-order nonlinear, linear, as well as total OAC within a GaAs/AlGaAs QD in the presence of an applied external electric field. The following parameters are used for calculation, $m^* = 0.067m_0$, (where m_0 is the electron mass), $n_\mathrm{r} = 3.2$, $T_{12} = 0.2$ ps, $\Gamma_{12} = 1/T_{12}$, $\sigma_v = 5\times10^{24}$ m^{-3}, $\mu = 4\pi\times10^{-7}$ Hm^{-1}.[30,31]

Figure 1 shows the third-order nonlinear, linear, together with total OAC according to the incident photon energy.

Clearly, the third-order nonlinear, linear, as well as total OAC get a resonant peak at the same location. The linear part of the OAC occupies a prominent position. However, it is affected by the third-order nonlinear terms. Thus, the total OAC is reduced. It can also be found based on Figs. 2–6 that the total OAC can be adequately adjusted by the external electric field, parameters of Gaussian potential, the QD radius, and incident optical intensity.

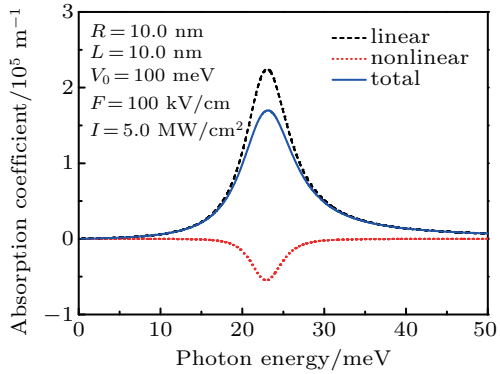

Fig. 1. The third-order nonlinear, linear, as well as total OAC based on incident photon energy at the parameters of $R = 10.0$ nm, $L = 10.0$ nm, $V_0 = 100$ meV, $F = 100$ kV/cm, $I = 5.0$ MW/cm^2.

Figure 2 displays the total OAC based on the incident photon energy with four distinct F values. As is observed, the OAC resonant peak elevates with the increase in F, suggesting the huge impact of electric field magnitude on the OAC resonant peak. For this feature, its physical origin is interpreted: when $z \ll L$, the Gaussian potential is the same as parabolic potential. For parabolic potential, the energy interval of the initial excited state compared with the system ground state does not change as the electric field changes.

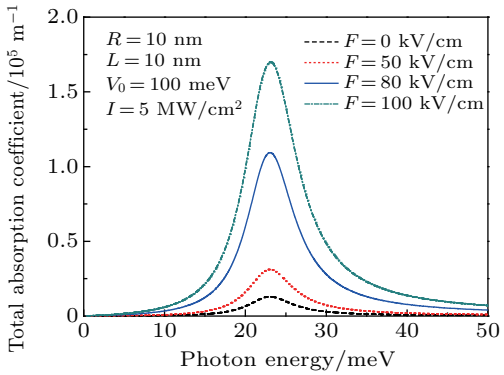

Fig. 2. The total OAC based on the incident photon energy at $R = 10.0$ nm, $L = 10.0$ nm, $V_0 = 100$ meV, $I = 5.0$ MW/cm^2 and four different values of F.

The total OAC based on the incident photon energy with four distinct L values is displayed in Fig. 3. Obviously, a broader range of the confinement potential leads to a larger resonant peak value. Additionally, as L elevates, the OAC resonant peak location remains unchanged.

For investigating quantum dot radius effect on the total OAC, we plot the total OAC based on the incident photon energy for three distinct R values. It can be known from Fig. 4 that the total OAC magnitude increases as the radius of QD decreases. The position of the resonant peak is another property, which obviously red shifts as the QD radius elevates, which is due to the weaker quantum confinement when QD radius increases. Therefore, difference in energy E_{21} between the system ground state and the initial excited state declines.

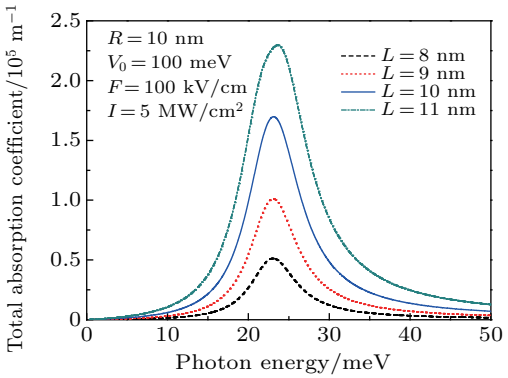

Fig. 3. The total OAC based on the incident photon energy at $R = 10.0$ nm, $V_0 = 100$ meV, $F = 100$ kV/cm, $I = 5.0$ MW/cm^2 and four different values of L.

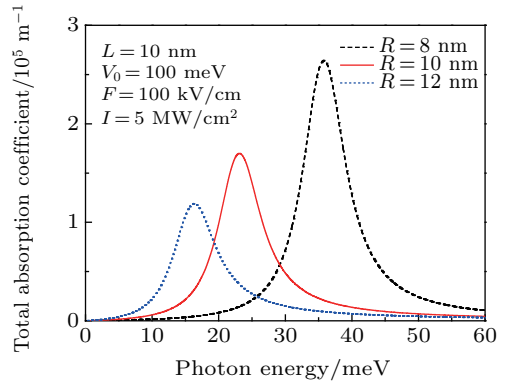

Fig. 4. The total OAC based on the incident photon energy at $L = 10.0$ nm, $V_0 = 100$ meV, $F = 100$ kV/cm, $I = 5.0$ MW/cm^2 and three different values of R.

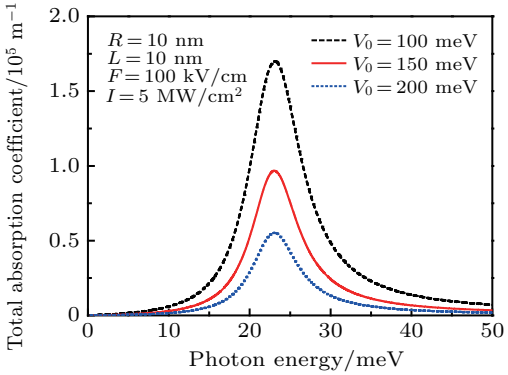

Fig. 5. The total OAC based on the incident photon energy at $R = 10.0$ nm, $L = 10.0$ nm, $F = 100$ kV/cm, $I = 5.0$ MW/cm^2 and three distinct values of V_0.

Figure 5 presents the total OAC according to the incident photon energy for three distinct V_0 values. It clearly seems that with the depth of Gaussian potential V_0 decreasing, the peak value of total OAC increases. As is observed, the total OAC peak position remains unchanged as the V_0 magnitude changes.

Total OAC based on the incident photon energy with three distinct I values is illustrated in Fig. 6. From the figure, it can be clearly noticed that, a higher incident optical intensity I results in a smaller total OAC. In addition, those resonant peaks of the total OAC are divided to two peaks at an incident optical intensity I of 15 MW/cm^2. The reason is that the third-order OAC exerts an important part in the total OAC.

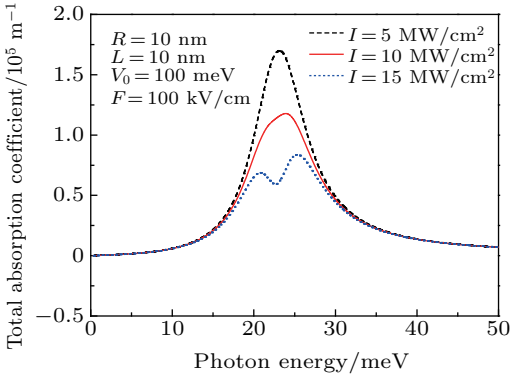

Fig. 6. The total OAC based on the incident photon energy at $R = 10.0$ nm, $L = 10.0$ nm, $V_0 = 100$ meV, $F = 100$ kV/cm and three distinct values of I.

4. Conclusions

In this paper, the OAC in the QD is effectively investigated. Our calculations mainly concentrate on the OAC dependency on the electric field F, the QD radius R, Gaussian potential V_0 and L parameters, and incident optical intensity I. According to our findings, the OAC theoretical value markedly elevates because of the Gaussian potential range and the electric field applied, but the peak value will decrease as the R, V_0 and I increase. Moreover, with the QD radius increasing, the resonant peaks of the OAC shift toward lower energy area. Our results are more remarkable than those in the previous work.[19] Hopefully, this research can provide certain foundation for experimental and theoretical work on optical devices.

References

[1] Rossetti R, Nakahara S and Brus L E 1983 *J. Chem. Phys.* **79** 1086
[2] Murray C B, Norris D J and Bawendi M G 1993 *J. Am. Chem. Soc.* **115** 8706
[3] Chang K and Xia J B 1998 *J. Appl. Phys.* **84** 1454
[4] Chang K and Xia J B 1998 *Phys. Rev. B* **57** 9780
[5] Chang K and Xia J B 1997 *Solid State Commun.* **104** 351
[6] Li S S, Chang K and Xia J B 2005 *Phys. Rev. B* **71** 155301
[7] Zhang C J, Min C and Zhao B 2019 *Phys. Lett. A* **383** 125983
[8] Çakır B, Yakar Y and Özmen A 2012 *J. Lumin.* **132** 2659
[9] Zhang C J and Liu C P 2019 *Opt. Express* **27** 37034
[10] Zhang C J and Liu C P 2019 *Laser Phys. Lett.* **17** 125401
[11] Bejan D 2016 *Phys. Lett. A* **380** 3836
[12] Ju K K, Guo C X and Pan X Y 2017 *Chin. Phys. B* **26** 097103
[13] Bahramiyan H 2018 *Opt. Mater.* **75** 187
[14] Kasapoglu E, Ungan F, Duque C A, Yesilgul U, Mora-Ramos M E, Sari H and Sökmen I 2014 *Physica E* **61** 107
[15] Sari H, Yesilgul U, Ungan F, Sakiroglu S, Kasapoglu E and Sökmen I 2017 *Chem. Phys.* **487** 11
[16] Aalu B 2019 *Physica B* **575** 411699
[17] Mandal A, Sarkai A, Ghosh A P and Ghosh M 2015 *Chem. Phys.* **463** 149
[18] Zhang Z Z, Zou L L, Liu C L and Yuan J H 2015 *Superlatt. Microstruct.* **85** 385
[19] Çakır B, Yakar Y and Özmen A 2017 *Physica B* **510** 86
[20] Ghajarpour N S and Karimi M J 2018 *Opt. Mater.* **82** 75
[21] Al E B, Kasapoglu E, Sakiroglu S, Duque C A and Sökmen I 2018 *J. Mol. Struct.* **1157** 288
[22] Zhang C J and Liu C P 2016 *Phys. Lett. A* **380** 3233
[23] Chen Y Y, Feng X L and Liu C P 2016 *Phys. Rev. Lett.* **117** 023901
[24] Zhang C J, Wu E, Gu M L, Hu Z F and Liu C P 2017 *Phys. Rev. A* **96** 033854
[25] Zhang C J, Wu E, Gu M L, Hu Z F and Liu C P 2017 *Opt. Express* **25** 21241
[26] Xie W F 2004 *Commun. Theor. Phys.* **42** 151
[27] Wu J H, Guo K X and Liu G 2014 *Physica B* **446** 59
[28] Kırak M, Yılmaz S, Şahin M and Gençaslan M 2011 *J. Appl. Phys.* **109** 094309
[29] Karimi M J, Keshavarz A and Poostforush A 2011 *Superlatt. Microstruct.* **49** 441
[30] Guo A X and Du J F 2013 *Superlatt. Microstruct.* **64** 158
[31] Ungan F, Restrepo R L, Mora-Ramos M E, Morales A L and Duque C A 2014 *Physica B* **434** 26